Equation of State from Potts-Percolation Model of a Solid

Miron Kaufman, Hung The Diep

Equation of State from Potts-Percolation Model of a Solid

Miron Kaufman[a] and H. T. Diep[b*]

[a] *Department of Physics,*

Cleveland State University,

Cleveland, OH 44115, USA

[b] *Laboratoire de Physique Théorique et Modélisation,*

Université de Cergy-Pontoise,

CNRS, UMR 8089

2, Avenue Adolphe Chauvin,

95302 Cergy-Pontoise Cedex, France

We expand the Potts-percolation model of a solid to include stress and strain. Neighboring atoms are connected by bonds. We set the energy of a bond to be given by the Lennard-Jones potential. If the energy is larger than a threshold the bond is more likely to fail, while if the energy is lower than the threshold the bond is more likely to be alive. In two dimensions we compute the equation of state: stress as function of inter-atomic distance and temperature by using renormalization group and Monte Carlo simulations. The phase diagram, the equation of state, the isothermal modulus and the thermal expansion are determined. When the Potts heat capacity is divergent the continuous transition is replaced by a weak first-order transition through the van der Waals loop mechanism. When the Potts transition is first order the stress exhibits a large discontinuity as function of the inter-atomic distance.

PACS numbers: 05.10.Ln,05.10.Cc,62.20.-x

* Corresponding author, E-mail:diep@u-cergy.fr

I. INTRODUCTION

The mechanical properties of solids, such as the mechanical failure, are topics of considerable interest[1–4]. In this paper we continue the analysis of an equilibrium statistical mechanics model[5,6] of a solid. Previously we assumed[7] harmonic springs and evaluated the role of thermal fluctuations by using renormalization-group and Monte-Carlo simulations. Furthermore we studied[8] the model with an extended defect line and found a hybrid, first- and second-order phase transition. In this paper we study the equation of state of the solid, stress as function of strain and temperature, obtained by assuming neighboring atoms are separated by a fixed inter-atomic distance and associating to each pair of neighboring atoms the Lennard-Jones energy. An alternative realistic anharmonic energy versus atomic distance due to Ferrante[9] has been considered in a previous work[10].

The model is defined in Section II. We assume the energy of a pair of neighboring atoms to be given by the Lennard-Jones 6-12 potential. If the energy of such a spring is larger than the threshold energy, the probability for its failure is higher than 50%. This model is mapped into a Potts model with couplings that are dependent on the inter-atomic distance. The free energy, number of live bonds, their fluctuations, stress, modulus and thermal expansion are computed using renormalization group and Monte Carlo techniques.

The equation of state is studied paying particular attention to the solid failure signaled by an extremum in the dependence of stress on the inter-atomic distance. Beyond the maximum under expansion and the minimum under compression for stress versus strain dependence, the solid ceases to be thermodynamically stable. The phase diagram includes the Potts transition line. If the Potts transition line is in the stable region of the phase diagram and if the q value is such that the Potts heat capacity is divergent, a remarkable phenomenon occurs in the vicinity of the transition line. A van der Waals loop[11] developes in the stress-strain dependence signaling a weak phase transition that replaces the continuous Potts phase transition. While in the renormalization group calculations[12,13] that are exact[14] on hierarchical lattices[15,16],the Potts transitions are always continuous, in the Monte Carlo simulations we can see both continuous transitions, for small q, and discontinuous transitions, for large q. This allows us to explore the influence of the order of the Potts transition on the mechanical properties of the solid, such as stress dependence on temperature and interatomic distance.

In Section III we present numerical results based on the renormalization-group Migdal-Kadanoff scheme. Monte-Carlo simulations are presented in Section IV. Our concluding remarks are found in Section V.

II. MODEL

The energy of any pair of neighboring atoms is:

$$E(r) = \epsilon[(\frac{r_0}{r})^{12} - 2(\frac{r_0}{r})^6] \tag{1}$$

where r is the inter-atomic distance and r_0 is the equilibrium inter-atomic distance (under zero stress). If the energy of the spring is larger than the threshold energy E_0 the bond is more likely to fail than to be alive. p is the probability that the bond is alive and $1-p$ the probability that the bond is broken. We assume the probabilistic weight $w = p/(1-p)$ to depend on energy through the Boltzmann weight:

$$w = \frac{p}{1-p} = e^{-\frac{E(r)-E_0}{k_B T}} \tag{2}$$

We allow for correlations between failing events by using the Potts number of states q, which plays the role of a fugacity controlling the number of clusters. For the same number of live bonds, graphs with more clusters are favored if $q > 1$, while if $q << 1$ there is a tendency to form a few large clusters. If $q = 1$ bonds fail independently of one another, i.e. random percolation process.

The partition function is obtained[17] by summing over all possible configurations of bonds arranged on the lattice

$$Z = \sum_{config} q^C w^B \tag{3}$$

C is the number of clusters, including single site clusters, and B is number of live bonds.

The free energy per bond is $f = \ln Z/N_{bonds}$. The derivatives of the free energy f with respect to w and q provide respectively the number of live bonds b and the number of clusters c, each normalized by the total number of lattice bonds

$$b \;=\; w\frac{\partial f}{\partial w} \tag{4}$$

$$c \;=\; q\frac{\partial f}{\partial q} \tag{5}$$

The derivatives of b and c with respect to w and q provide the fluctuations (variances) of those quantities:

$$\Delta b^2 \;=\; w\frac{\partial b}{\partial w} \tag{6}$$

$$\Delta c^2 \;=\; q\frac{\partial c}{\partial q} \tag{7}$$

The stress σ is calculated by taking the derivative of the free energy with respect to r, the inter-atomic distance:

$$\sigma = -k_B T\frac{\partial f}{\partial r} = b\frac{dE(r)}{dr} \tag{8}$$

The equation of state, Eq. (8), states that the average stress is equal to the stress associated with each live bond $dE(r)/dr$ multiplied by the number of live bonds b. The energy gradient is obtained from Eq. (1):

$$\frac{dE(r)}{dr} = -\frac{12\epsilon}{r_0}\left[(\frac{r_0}{r})^{13} - (\frac{r_0}{r})^{7}\right] \tag{9}$$

The equation of state yields the isothermal linear modulus (inverse compressibility) m and the coefficient of linear thermal expansion α:

$$m \;=\; \frac{\partial \sigma}{\partial r}|_T = \frac{d^2E(r)}{dr^2} - \frac{1}{k_B T}\Delta b^2(\frac{dE(r)}{dr})^2 \tag{10}$$

$$\alpha \;=\; \frac{\partial r}{\partial T}|_\sigma = -\frac{E(r)-E_0}{k_B T^2}\frac{dE(r)}{dr}\frac{1}{m}\Delta b^2 \tag{11}$$

We perform Monte Carlo simulations of the model using its mapping into the Potts model. By using the Kasteleyn-Fortuin expansion[18,19] we can rewrite the partition function, Eq. (3), as:

$$Z = Tr_\sigma e^{-\frac{H}{k_B T}} \tag{12}$$

The Hamiltonian is:

$$-\frac{H}{k_B T} = \sum_{<i,j>} J(r)\delta(s_i, s_j) \tag{13}$$

where s_i is a Potts[20] spin at the lattice site i taking q values. The coupling constant $J(r)$ is related to the original parameters by

$$J(r) = \ln(1+w) = \ln(1+e^{-\frac{E(r)-E_0}{k_B T}}) \tag{14}$$

To get the equation of state from Monte Carlo simulations for a given T, r, and E_0, we calculate the Potts coupling constant $J(r)$, using Eq. (14). Then we rewrite Eq. (8) to get the stress. The number of live bonds b is obtained from the Potts energy

$$u = -\overline{\delta(s_i, s_j)} \tag{15}$$

The equation of state becomes

$$\sigma = -u[e^{\frac{E(r)-E_0}{k_B T}} + 1]^{-1} \frac{dE(r)}{dr} \tag{16}$$

In all numerical results that will be presented next in Section III from renormalization group calculations and in Section IV from Monte Carlo simulations, we express energy in units of ϵ, temperature in units of ϵ/k_B, distance in units of r_0 and stress in units of ϵ/r_0.

III. RENORMALIZATION GROUP

The Migdal-Kadanoff[12,13] recursion equation for two dimensions is

$$w' = [1 + \frac{w^2}{2w+q}]^2 - 1 \tag{17}$$

The free energy $f = \ln Z/N_B$, N_B being the number of lattice edges, is

$$f = \sum_N \frac{C_N}{4^N} \tag{18}$$

where

$$C = 2\ln(2w+q) \tag{19}$$

The recursion equations (17)-(19) represent the exact solutions[14] for the diamond hierarchical lattice[15,16].

The renormalization group flows are governed by the following fixed points: i. $w = 0$ (non-percolating live bonds), ii. $w = \infty$ (percolating network of live bonds), iii. $w = w_c$ (Potts critical point). Using the free energy we can compute the number of live bonds b, their

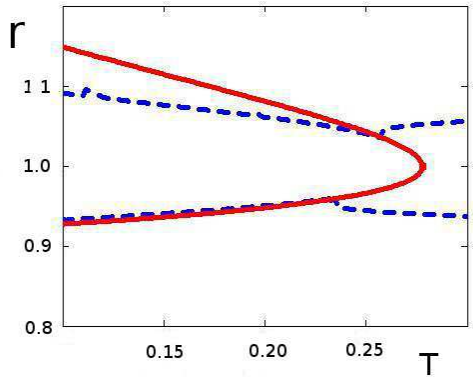

FIG. 1: Phase diagram (T, r) plane for $E_0 = -0.5$, $q = 10$. Dashed (blue) lines are instability lines and solid (red) line is Potts transition line.

fluctuation (variance), stress, thermal expansion and modulus. Each of those quantities is scaled by the total number of lattice bonds.

For given values of E_0 and q, the phase diagram in the plane (T, r) includes two type of singularity lines. In Fig. 1 we fixed the threshold energy at $E_0 = -0.5$ and the clusters fugacity at $q = 10$. The Potts- percolation line separates the region where the probability for formation of an infinite cluster of live bonds is non-zero from the region where the probability is zero. On this line the probability weight defined in Eq. (2) is equal to w_c. On the instability line the solid becomes soft, as its modulus vanishes $\partial\sigma/\partial r = 0$. The minimum of stress versus inter-atomic distance under compression ($r < 1$) and its maximum under expansion ($r > 1$) provide the limits of stability for the solid. The solid becomes soft at these points. Beyond this line the solid is thermodynamically unstable since $\partial\sigma/\partial r < 0$. Note that a large portion of the Potts transition line (solid,red) is situated in the unstable region.

We show in Fig. 2 the stress versus inter-atomic distance for two isotherms $T = 0.2$ and $T = 0.26$ respectively. The modulus and the thermal expansion are shown in Fig. 4 for the

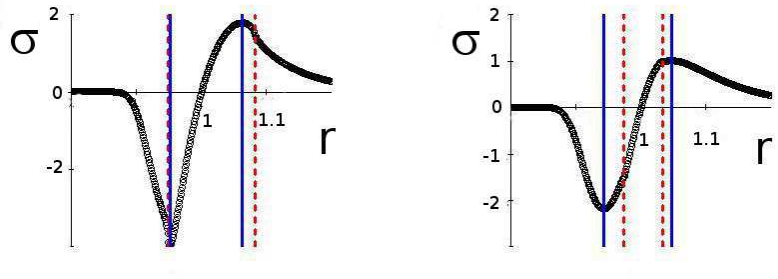

FIG. 2: Equation of state isotherms: stress versus strain for $E_0 = -0.5$, $q = 10$, $T = 0.2$ (left) and 0.26 (right). The Potts critical points are indicated by the dashed lines and the stability limits are indicated by the solid lines. In Fig. 3 we show zooms close to the Potts critical points.

same values of the model parameters.

The $T = 0.2$ isotherm is in the region of phase diagram where the Potts transition is in the instability region while the $T = 0.26$ one is in the region where the Potts transition is in the stable region. A zoom view on the isotherm $T = 0.26$ in the neighborhoods of the two Potts transitions (see Fig. 3) reveals van der Waals loops[11] that yield weak discontinuous transitions (small discontinuity) by means of the Maxwell construction. Hence discontinuous transitions replace the continuous transition of the Potts model for the hierarchical lattice. The modulus and the thermal expansion (Fig. 4) show anomalies at the Potts transition that are connected to the divergence of Δb^2 (or of the heat capacity) in the Potts model on the diamond hierarchical lattice for $q = 10$. The modulus becomes negative, and thus the solid is thermodynamically unstable, when Δb^2 is large enough, see Eq. (8). For the square lattice we expect the same phenomenon for $q = 2, 3, 4$ where the heat capacity (and thus Δb^2) is infinite at the Potts critical point. This will be confirmed through Monte Carlo simulations in Sec IV below.

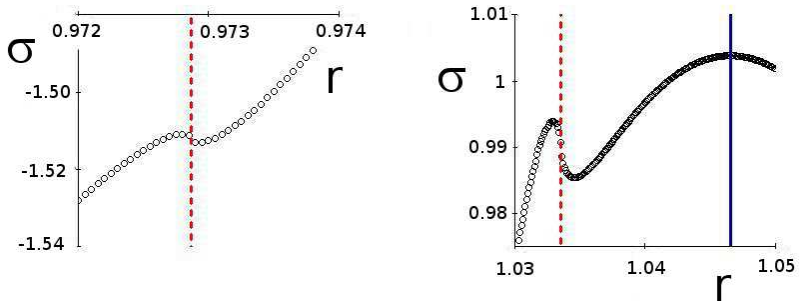

FIG. 3: Close-ups on isotherm $E_0 = -0.5$, $q = 10$, $T = 0.26$ near the Potts transition line under compression and expansion, respectively. van der Waals loops, that signal discontinuous transitions through the Maxwell construction, are exhibited at the Potts critical points (indicated by dashed lines). The solid line shows the stability limit.

In Fig. 5 we show the isotherm where the temperature equals the critical temperature for $r = 1$ (equilibrium inter-atomic distance for zero stress). We also show the corresponding modulus. The anomaly apparent in Figs. 2-4 is not present at $r = 1$ because the derivative of E with respect to r [see Eq. (9)] is zero at $r = 1$ and thus the negative contribution on the right hand side of Eq. (10) vanishes.

To illustrate the dependence of the phase diagram on the parameters q and E_0 we show, beside the phase diagram for $E_0 = -0.5$, $q = 10$ of Fig. 1, the phase diagram for $E_0 = 0.5$, $q = 10$ in Fig. 6, and the phase diagrams for $E_0 = -0.5$, $q = 1$, and for $E_0 = 0.5$, $q = 1$ in Fig. 7. The Potts line in the (T, r) plane is obtained by substituting in Eq. (2) the critical value $w_c(q)$, $r_0 = 1$ and using Eq. (1):

$$(\frac{1}{r})^{12} - 2(\frac{1}{r})^{6} = E_0 - T\ln(w_c(q)) \tag{20}$$

For the self-dual square lattice the critical value[18] is $w_c(q) = \sqrt{q}$ and this will be used

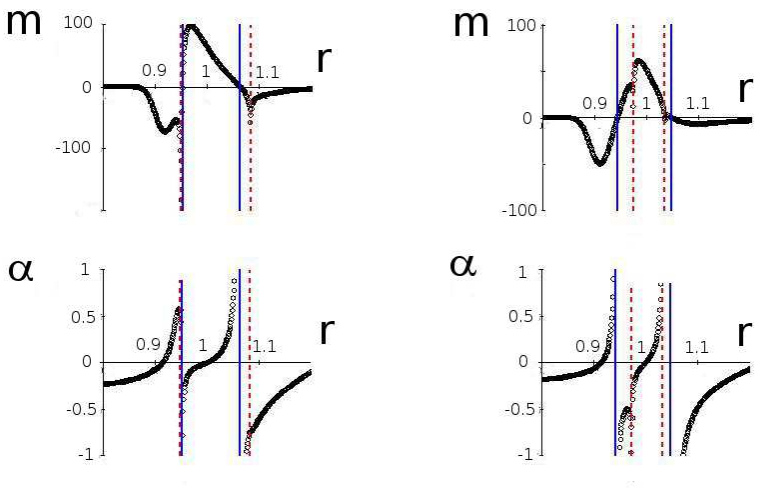

FIG. 4: Isothermal modulus and thermal expansion versus inter-atomic distance for $E_0 = -0.5$, $q = 10$, $T = 0.2$ (left) and 0.26 (right). The Potts transitions are indicated by the dashed lines, while the solid lines show the stability limits.

in Sec.IV below to verify the accuracy of the Monte Carlo simulations. The instability line originates at zero temperature at the two values of r for which $E(r) = E_0$ provided the the threshold energy is $-1 < E_0 < -0.787$. The energy value of -0.787 is the energy at the inflexion point $r = 1.11$. If the threshold energy $E_0 > -0.787$ the instability line in the expansion region $r > 1$ originates from the inflexion point of $E(r)$, while under compression the starting point is at the r for which $E(r) = E_0$.

IV. MONTE CARLO SIMULATIONS

A. General remarks

We perform here Monte Carlo simulations using Eq. (13) with the nearest-neighbor interaction $J(r)$ given by Eq. (14). For a given q, the main parameters are T, r and E_0. As in the previous section, we fix q and E_0 and make simulations in the space (T, r).

The details of the simulations are the following. We consider a square lattice of size

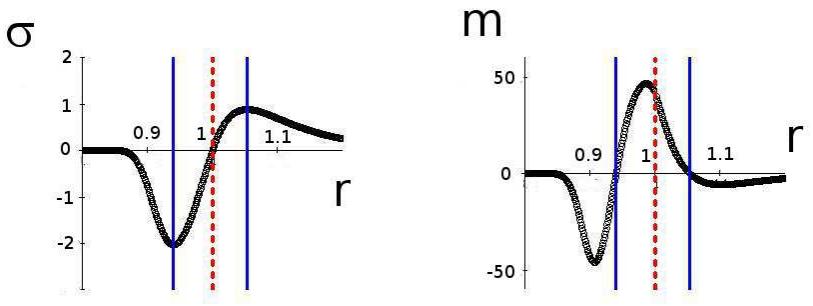

FIG. 5: Stress and modulus versus inter-atomic distance at the critical temperature corresponding to $r = 1$. The Potts critical point is indicated by the dashed line. No anomaly occurs because of the vanishing of $\frac{dE}{dr}$. The solid lines show the stability limits.

$N_x \times N_y$ where $N_x = N_y = 40, 60, 80, 100$. Each lattice site is occupied by a $q-$state Potts spin. We use periodic boundary conditions. Depending on the location of the studied point in the phase space, we used an equilibrating time from 10^5 to 10^6 MC steps per spin and an averaging time of the order of 10^6 MC steps per spin.

One purpose here is to test the renormalization group prediction of section III for the cases when the heat capacity of the Potts model is divergent at criticality: $q = 2, 3, 4$. Though the renormalization group analysis is exact for diamond hierarchical lattice, its predictions for the square lattice are to be checked. The other goal of the simulations is to learn about the influence of the discontinuous Potts transition for $q > 4$ on the equation of state of our model. To achieve this we simulate the $q = 10$ on the square lattice.

To verify the accuracy of our simulations we compared the critical temperature estimated from our simulations to the exact critical temperature. For $r = 1$ it is:

$$T_c = \frac{1 + E_0}{\ln(\sqrt{q})} \tag{21}$$

With $q = 4$, $E_0 = -0.5$, we find $T_c \simeq 0.721$. The Monte Carlo simulations give the same

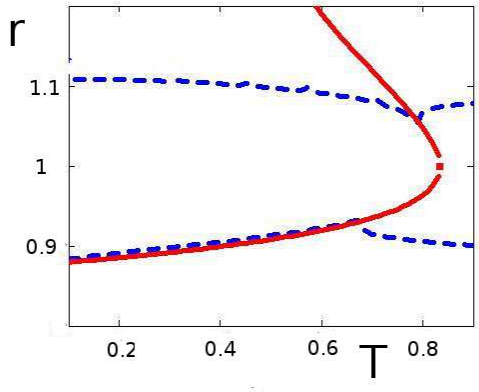

FIG. 6: Phase diagram (T, r) plane for $E_0 = 0.5$, $q = 10$. Dashed (blue) lines are instability lines and the solid (red) line is the Potts transition line.

result up to 4 digits.

In MC simulations, we work at finite sizes, so for each size we have to determine the "pseudo" transition which corresponds in general to the maximum of the specific heat or of the susceptibility. The maxima of these quantities need not to be at the same temperature. Only at the infinite size, they should coincide. The theory of finite-size scaling permits to deduce properties of a system at its thermodynamic limit. We have used in this work a size large enough to reproduce the bulk transition temperature up to the fourth decimal. We define the Potts order parameter Q by

$$Q = [q \max(Q_1, Q_2, ..., Q_q) - 1]/(q - 1) \tag{22}$$

where $Q_n (n = 1, ..., q)$ is the averaged value defined by

$$Q_n = < \sum_j \delta(s_j - n)/(N_x N_y) > \tag{23}$$

s_j being the Potts spin at the site j.

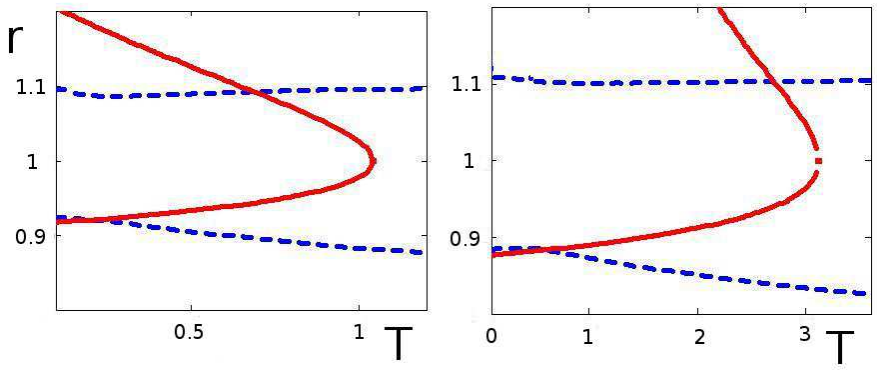

FIG. 7: Phase diagram (T, r) plane for $E_0 = -0.5$ (left) and $E_0 = 0.5$ (right) for $q = 1$. Dashed (blue) lines are instability lines and solid (red) line is Potts transition line.

B. Results for q=10

We recall that the Potts model shows a first-order transition[18] for $q > 4$ at a finite temperature. This is seen in Fig. 8 where the averages of the energy per spin E defined by the statistical average of the right-hand side of Eq. (13) and the Potts energy U defined by Eq. (15) are shown for three values of r.

Note that these energies show a large discontinuity at the transition temperature. Fig. 9 shows the order parameter at three values of r as a function of T. Again here, a huge discontinuity is seen. These results confirm the first-order character of the transition. Repeating the simulations for other values of r, we determine the Potts transition line in the space (T, r) which is shown in Fig. 10. We have compared the exact critical line of Eq. (20), using $w_c = \sqrt{10}$, to the Monte-Carlo simulations estimates to ascertain the reliability of our numerics. Note that unlike in some first-order transitions, the slow heating and slow cooling of the system do not result in a hysteresis. The energy barrier between the two phases is believed to be therefore not so high.

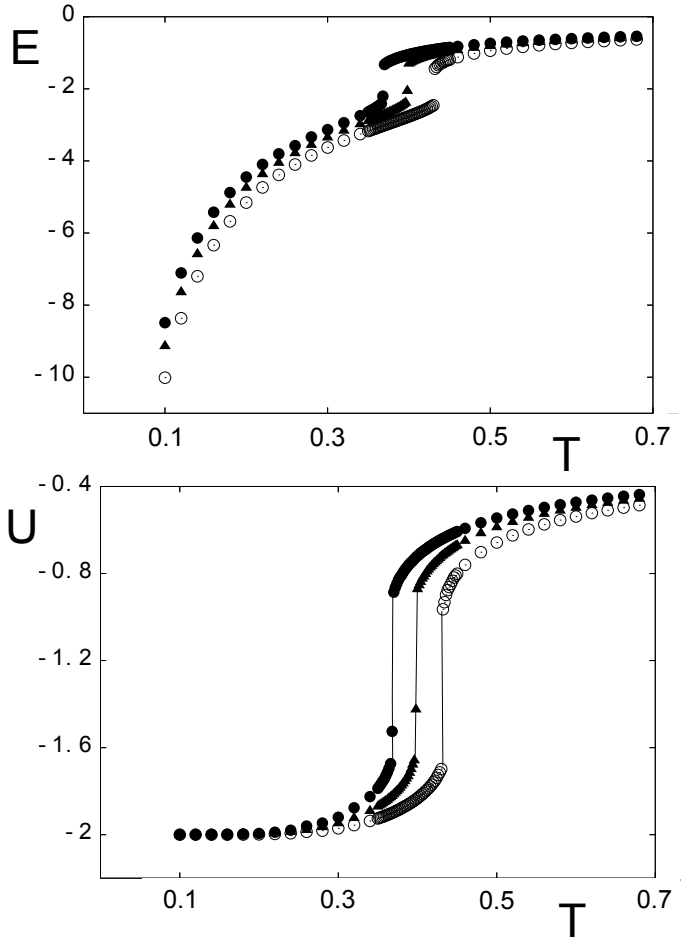

FIG. 8: Averaged energy per spin E (upper) and averaged Potts energy U (lower) vs temperature T for $q = 10$, $r = 0.96$ (black circles), 1 (void circles), and 1.04 (black triangles), with $N_x = N_y = 100$ and $E_0 = -0.5$. Lines are guides to the eye.

We calculate the stress σ using the Eq. (16) with u obtained from MC simulations shown above in Fig. 8, $E(r)$ and $dE(r)/dr$ being given by Eqs. (1) and (9). This is done for many values of r and T around the Potts transition curve in search for unstable regions predicted by the RG analysis shown in Figs. 1-6. In practice, we fixed a temperature and then changed the value of r across the Potts transition line by following a vertical line in Fig. 10. In doing so, we obtained for each T the stress as a function of r. At a given T, if there is no crossing of the Potts transition line then the stress behaves as shown in the curve for $T = 0.46$ in Fig. 11: σ goes smoothly through a minimum at a compression position to a maximum at a dilatation one. The solid is stable in the region between the minimum and the maximum since the modulus $d\sigma/dr$ is positive. On the other hand, when

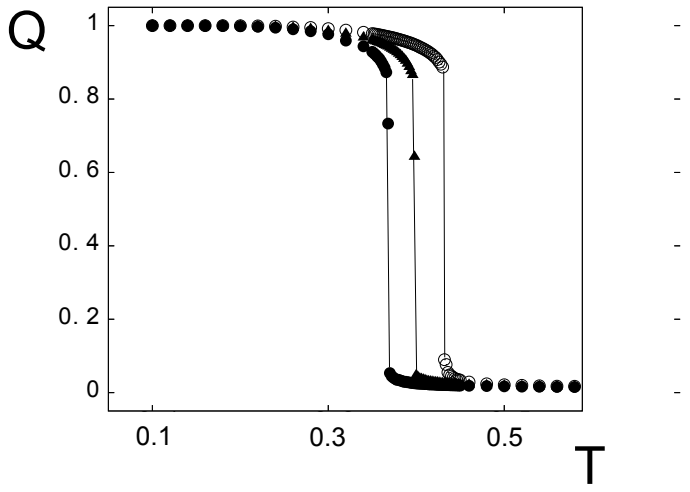

FIG. 9: Order parameter Q versus temperature T for $q = 10$, $r = 0.96$ (black circles), 1 (void circles), and 1.04 (black triangles), with $N_x = N_y = 100$ and $E_0 = -0.5$. Lines are guides to the eye.

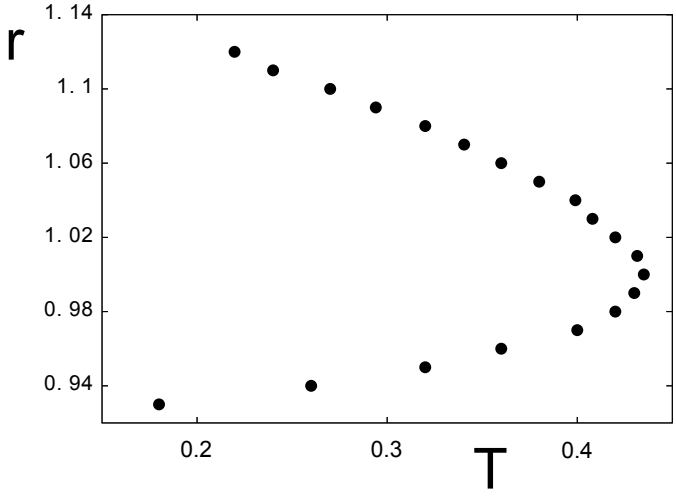

FIG. 10: Phase diagram of the Potts transition in the space (T, r) for $q = 10$, with $N_x = N_y = 100$ and $E_0 = -0.5$.

the system crosses the transition line by varying r, the stress exhibits jumps as seen in the three curves at $T = 0.36$, 0.38, 0.40 in Fig. 11. These transition points lie on the Potts transition line shown in Fig. 10. The discontinuity in stress is due to the Potts energy discontinuity associated with the first-order transition of the 10-state Potts model. The first-order nature in the case $q = 10$ observed above enhances the instability. As will be seen below, a qualitatively different instability occurs for $q = 2, 3, 4$ where the transition is

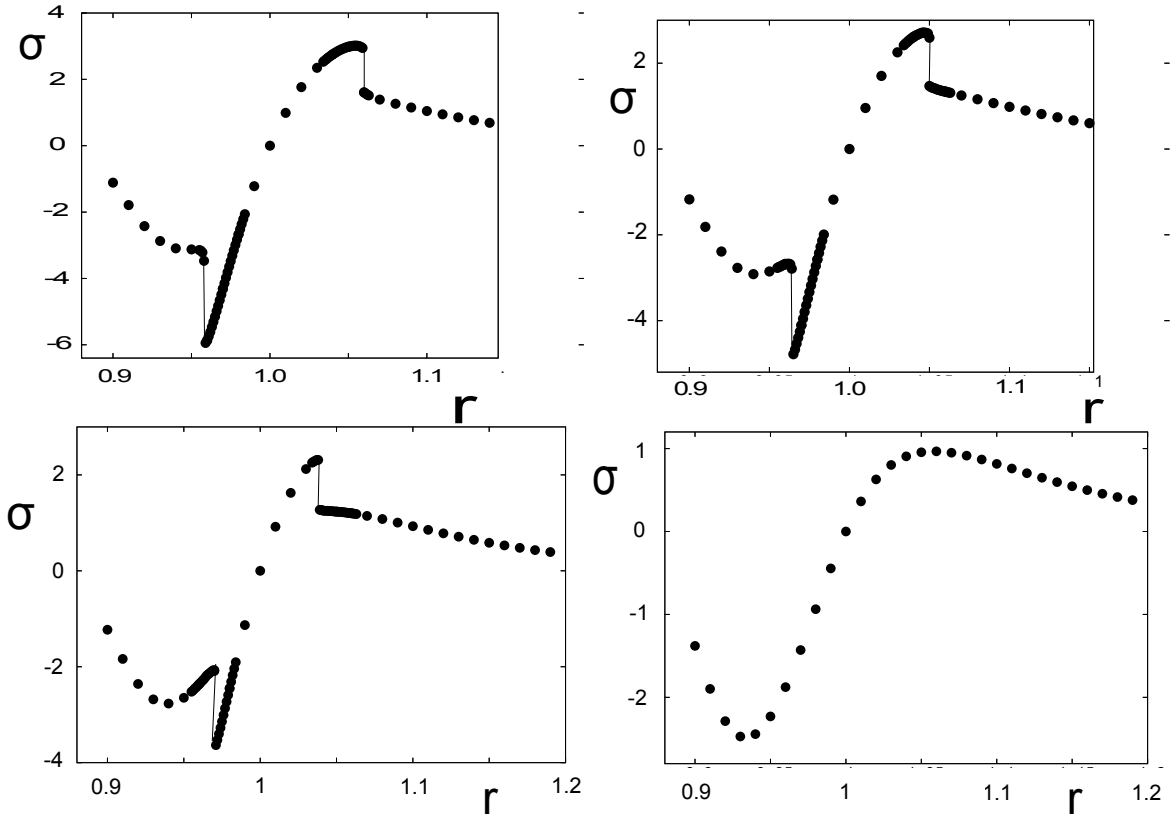

FIG. 11: Stress vs r for $q = 10$ at $T = 0.36$ (upper left), 0.38 (upper right), 0.40 (lower left), 0.46 (lower right), with $N_x = N_y = 100$ and $E_0 = -0.5$. Lines are guides to the eye. See text for comments.

of second order.

It is interesting to show now in Fig. 12 the stress versus T at a given r. As seen the stress undergoes a discontinuity at the Potts transition temperature if $r \neq 1$, but the discontinuity vanishes for $r = 1$.

To close this sub-section, we emphasize that for the system studied here, the size effects are indistinguishable from $N_x = N_y = 60$ up.

C. Results for q = 2, 3, 4

Let us consider the case where $q = 4$. We show in Figs. 13 and 14 the averaged energy per site [Eq. (13)], the averaged Potts energy [Eq. (15)] and the order parameter Q obtained by MC simulations as described above for $q = 4$, $E_0 = -0.5$ and three values of r. The Potts transition is of second order as expected[18].

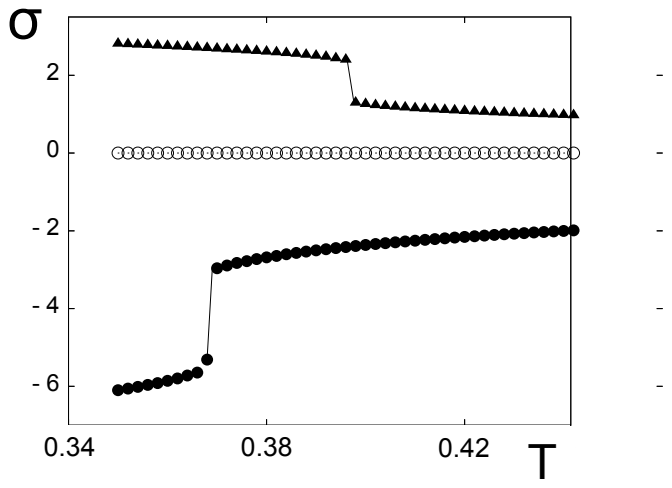

FIG. 12: Stress vs T for $q = 10$, at three values of r: r=1.04 (black triangles), 1 (void circles) and 0.96 (black circles), with $N_x = N_y = 100$ and $E_0 = -0.5$. Note the discontinuities in the cases $r = 0.96$ and 1.04. Lines are guides to the eye. See text for comments.

Performing simulations for a large range of r around $r_0 = 1$, one obtains the phase diagram shown in Fig. 15. We have compared the exact critical line of Eq. (20), using $w_c = \sqrt{4}$, to the Monte-Carlo simulations estimates to ascertain the reliability of our numerics.

We show in Fig. 16 an example of the instability taking place at the two Potts transitions. The zooms show very small van der Waals loops. At some other transitions (not shown) we observed also the same weak instability behavior in intensity.

For $q = 3$, the results are shown in Figs. 17-20. The second-order transition is observed here as expected.

The phase diagram shown in Fig. 19 has the same shape as the previous cases. We have compared the exact critical line of Eq. (20), using $w_c = \sqrt{3}$, to the Monte-Carlo simulations estimates to ascertain the reliability of our numerics. The stress always shows an instability at the phase transition. We show in Fig. 20 the stress at some temperatures at and near T_c. As seen, the van der Waals loops, though weak, are well present.

For $q = 2$, the results are shown in Figs. 21-23. All the curves have the same properties as those of the cases $q = 3, 4$: second-order transition with instability in the critical temperature region.

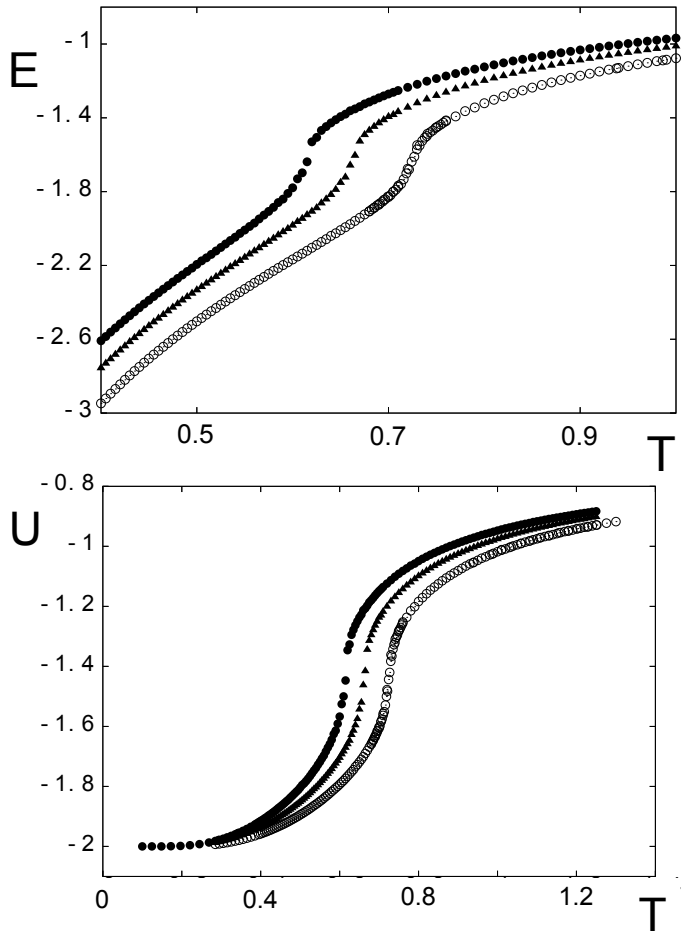

FIG. 13: Averaged energy per spin E (upper) and averaged Potts energy (lower) vs temperature T for $q = 4$, $r = 0.96$ (black circles), 1 (void circles), 1.04 (black triangles), with $N_x = N_y = 100$ and $E_0 = -0.5$.

V. CONCLUSIONS

In this paper, we have used renormalization group and Monte Carlo simulations to study the phase diagram of a two-dimensional solid by using a model in which the interaction between neighboring atoms follows the Lennard-Jones potential. We have mapped the model into a q-state Potts model and investigated the effect of both a uniform compression and a uniform expansion of the volume of the solid. In the temperature, inter-atomic distance plane we find a line of Potts transitions and stability boundaries where the stress as a function of inter-atomic distance has an extremum. For the cases where the Potts heat capacity is divergent ($q = 2, 3, 4$ for the square lattice, $q > 6.8$ for the hierarchical diamond lattice) a van der Waals loop (instability) occurs close to the Potts transition and thus a weak first-

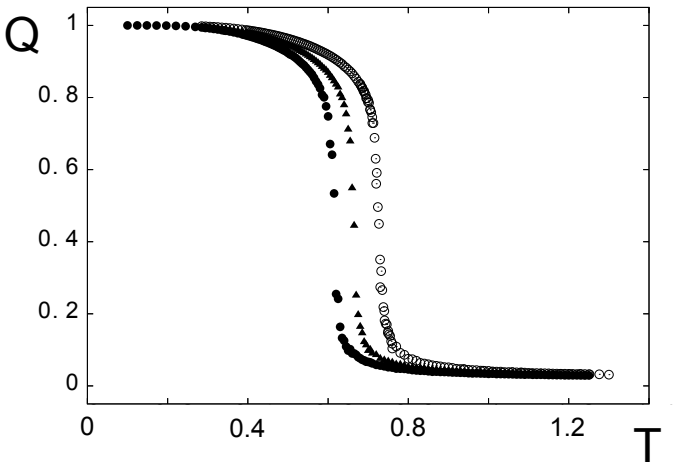

FIG. 14: Order parameter vs temperature T for $q = 4$, $r = 0.96$ (black circles), 1 (void circles), 1.04 (black triangles), with $N_x = N_y = 100$ and $E_0 = -0.5$.

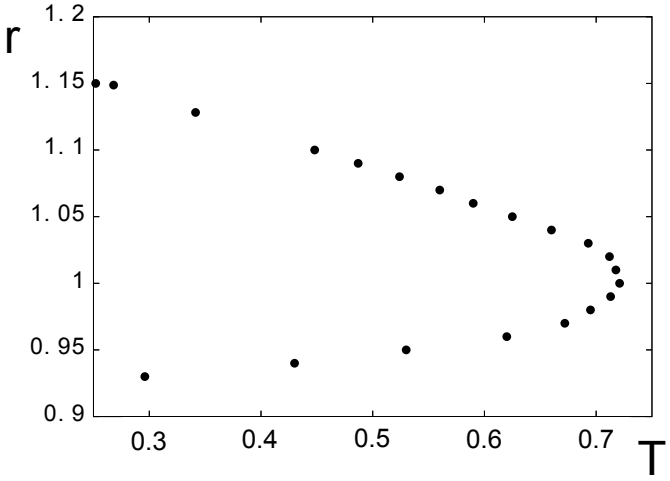

FIG. 15: Phase diagram of the Potts transition in the space (T, r) for $q = 4$, with $N_x = N_y = 100$ and $E_0 = -0.5$.

order transition (using Maxwell construction) replaces the continuous transition. This is a remarkable result that warrants further analysis. Monte Carlo simulations for large q values (where the square lattice Potts transition is discontinuous) indicate that the discontinuity in the Potts energy translates into a discontinuity in the stress as a function of the interatomic distance at the transition temperature. Finally, let us note that while it is known that the solid phase cannot survive at finite T in two dimensions with continuous degrees of freedom of atom motions, our present study with discrete degrees of freedom shows some interesting behaviors which would serve as a starting point to study three-dimensional solids where

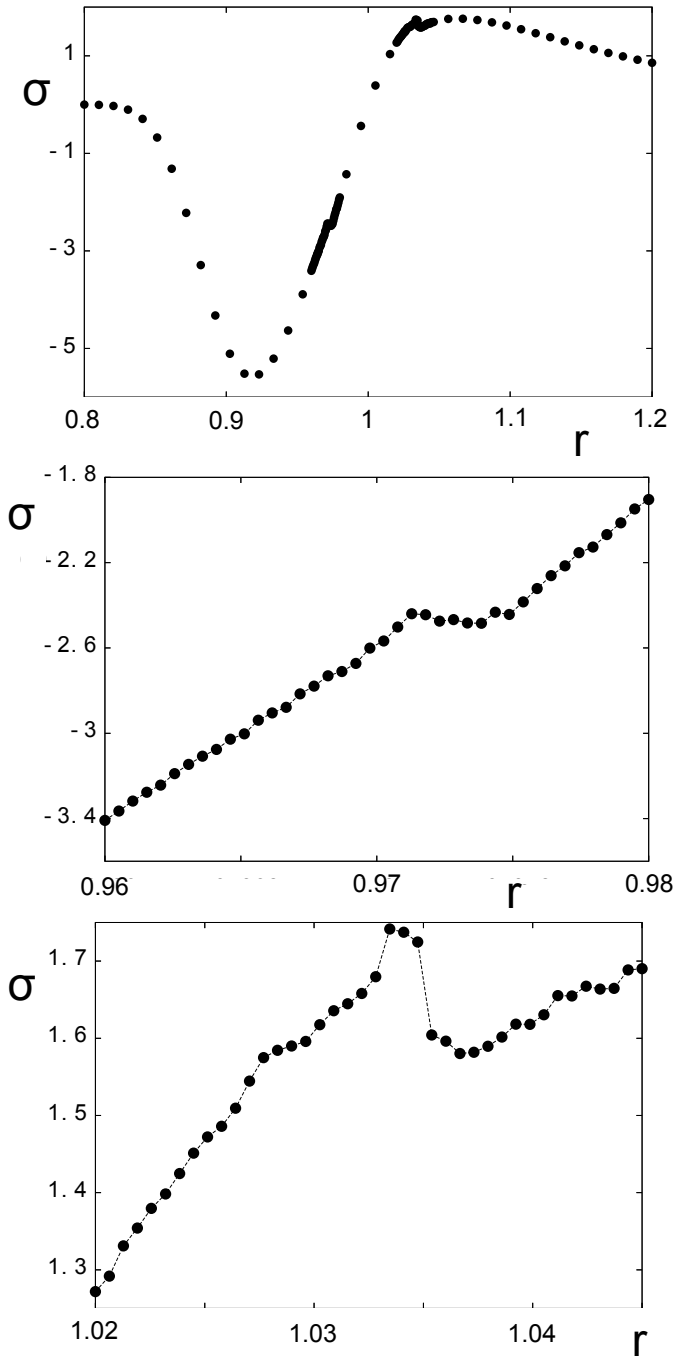

FIG. 16: Stress (upper curve) and zooms (lower curves) vs r for $q = 4$, $T = 0.67931$, with $N_x = N_y = 60$ and $E_0 = -0.5$.

melting mechanisms are not well understood.[21,22]

M.K. wishes to thank the University of Cergy-Pontoise for hospitality while this work

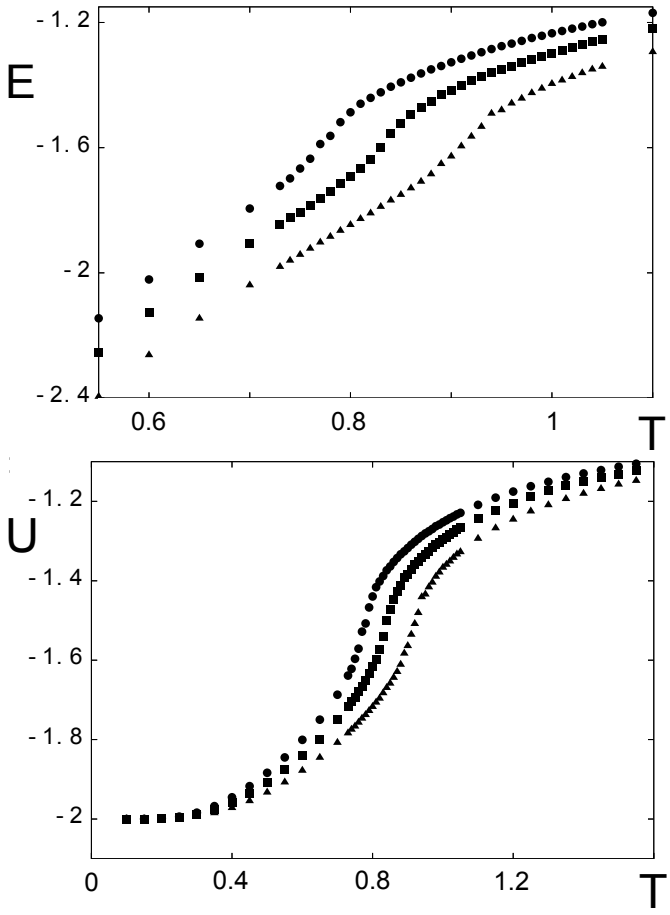

FIG. 17: Averaged energy per spin E (upper) and averaged Potts energy (lower) vs temperature T for $q = 3$, $r = 0.96$ (black circles), 1 (black triangles), 1.04 (black squares), with $N_x = N_y = 100$ and $E_0 = -0.5$.

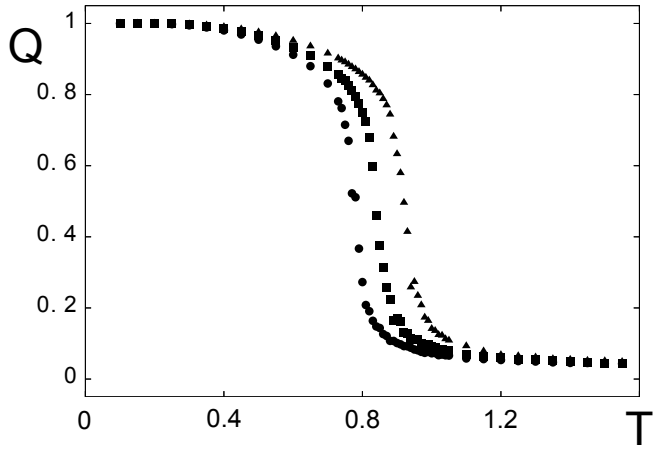

FIG. 18: Order parameter vs temperature T for $q = 3$, $r = 0.96$ (black circles), 1 (black triangles), 1.04 (black squares), with $N_x = N_y = 100$ and $E_0 = -0.5$.

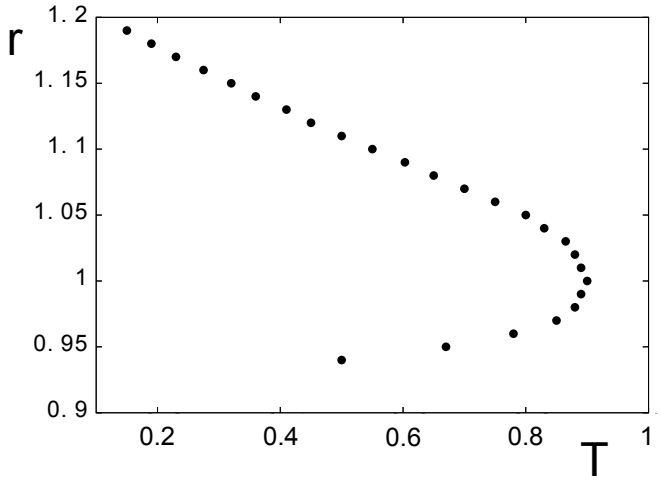

FIG. 19: Phase diagram of the Potts transition in the space (T, r) for $q = 3$, with $N_x = N_y = 100$ and $E_0 = -0.5$.

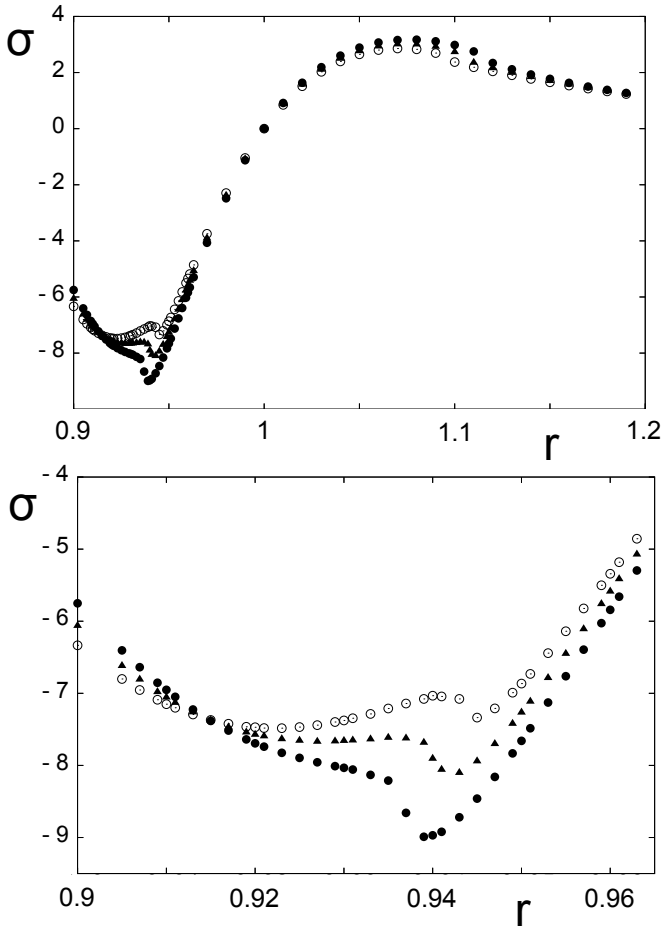

FIG. 20: Stress (upper) and zoom (lower) vs r for $q = 3$, $T = 0.5$ (black circles), 0.55 (black triangles) and 0.6 (void circles), with $N_x = N_y = 60$ and $E_0 = -0.5$.

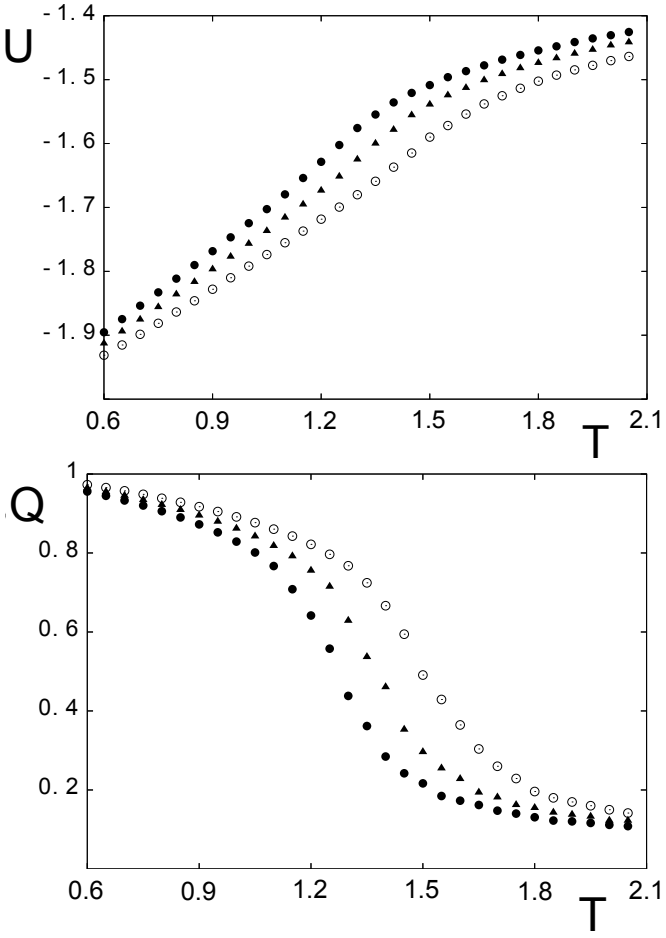

FIG. 21: Averaged Potts energy (upper) and order parameter (lower) vs temperature T for $q = 2$, $r = 0.96$ (black circles), 1 (void circles), 1.04 (black triangles), with $N_x = N_y = 100$ and $E_0 = -0.5$.

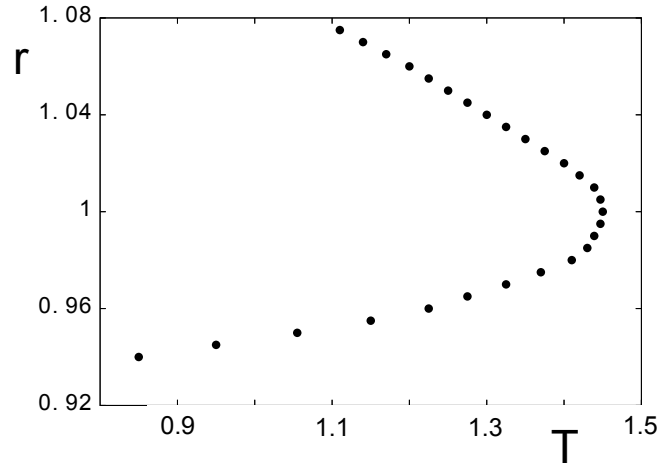

FIG. 22: Phase diagram of the Potts transition in the space (T, r) for $q = 2$, with $N_x = N_y = 100$ and $E_0 = -0.5$.

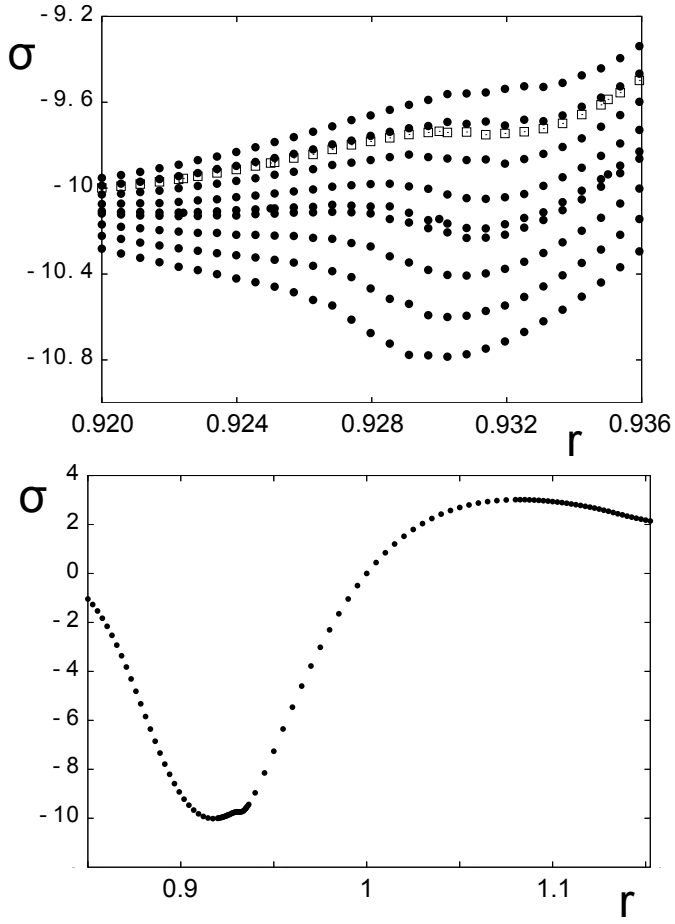

FIG. 23: Stress vs r near the instability region (upper) for $q = 2$ with several temperatures from $T = 0.535$ to 0.675: data points for $T = 0.65$ are marked with void squares. This case is shown for a large region of r in the lower figure. $N_x = N_y = 60$, $E_0 = -0.5$.

was carried out.

---

[1] L. De Arcangelis, A. Hansen, H. J. Hermann and S. Roux, Phys. Rev. B**40**, 877 (1989).

[2] P. D. Beale and D. J. Srolovitz, Phys. Rev. B**37**, 5500 (1988).

[3] Z. G. Wang, U. Landman, R. L. Blumberg Selinger and W. M. Gelbart, Phys. Rev. B**44**, 378 (1991).

[4] M. J. Alava, P. K. V. V. Nukala, and S. Zapperi, Advances in Physics**55**, 349 (2006).

[5] R. Englman and Z. Jaeger, Physica A**168**, 655 (1990).

[6] R. L. Blumberg Selinger, Z. G. Wang, W. M. Gelbart and A. Ben-Shaul, Phys. Rev. A**43**, 4396

(1991).

[7] M. Kaufman and H.T. Diep, J. Phys.: Condens. Matter **20**, 075222 (2008).

[8] H.T. Diep and M. Kaufman, Phys Rev E**80**, 031116 (2009).

[9] J. Ferrante and J. R. Smith, Phys. Rev. B**31**, 3427 (1985).

[10] M. Kaufman and J. Ferrante, NASA Tech. Memo. 107112 (1996).

[11] J. D. van der Waals, *On the Continuity of the Gaseous and Liquid States* Dover Publications, (2004).

[12] A. A. Migdal, JETP (SovPhys)**42**, 743 (1976).

[13] L. P. Kadanoff, Ann. Phys.(NY) **100**, 359 (1976).

[14] A. N. Berker and S. Ostlund, J. Phys. C **12**, 4961-4975 (1979).

[15] M. Kaufman and R.B. Griffiths, Phys. Rev. B **30**, 244 (1984).

[16] R. B. Griffiths and M. Kaufman, Phys. Rev. B **26**, 5022 (1982).

[17] M. Kaufman and D. Andelman, Phys. Rev. B**29**, 4010-4016 (1984).

[18] F. Y. Wu, Rev. Mod. Phys. **54**, 235-268 (1982).

[19] C. M. Fortuin and P. W. Kasteleyn, J. Phys. Soc. Jpn. Supplm. **26**, 11 (1969).

[20] R. B. Potts, Proc. Camb. Phil. Soc. **48**, 106 (1952).

[21] L. Gomez, A. Dobry and H. T. Diep, Phys. Rev. B **63**, 224103 (2001).

[22] L. Gomez, A. Dobry, H. T. Diep, Ch. Geuting and L. Burakowsky , Phys. Rev. Lett. **90**, 095701 (2003).